Supporting Information

Direct Electrochemical Analysis in Seawater: Evaluation of Chloride and Bromide Detection

Yuqi Chen[1] and Richard Compton [2]*

Physical and Theoretical Chemistry Laboratory, Department of Chemistry, University of Oxford, South Parks Road, Oxford OX1 3QZ, UK, UK; yuqi.chen@sjc.ox.ac.uk

*Corresponding author:

Email: Richard Compton richard.compton@chem.ox.ac.uk

Phone: +44(0) 1865 275957

Fax: +44(0) 1865 275410

Contents

Section 1: The Electro-dissolution of a Au Electrode in ASW

Cyclic voltammetry was conducted using a Au electrode in ASW1 containing 0.571 M chloride and 0.84 M bromide. The potential sweep started at −0.45 V vs MSE, and swept towards 0.94 V before returning to −0.45 V at a scan rate of 20 mVs^{-1}, 20 such potential cycles were made in succession. The dissolved gold can be seen plated onto the surface of the counter electrode in Figure S 1 and led to the coloration of the solution (Figure S 2).

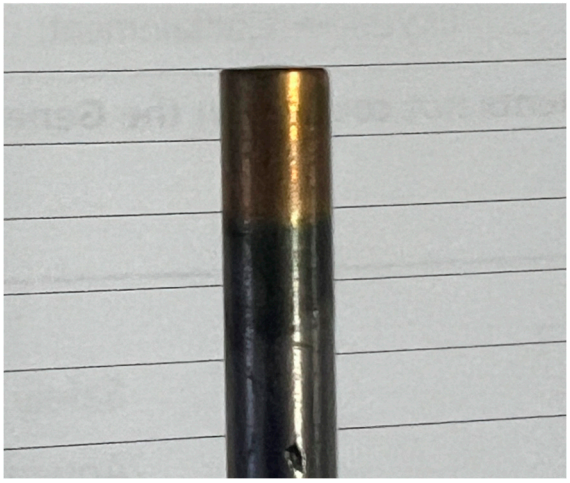

Figure S 1 A picture of the counter electrode after 20 scans of CV. The start potential was −0.45 V vs MSE and swept towards 0.94 V before returning to −0.45 V. The golden layer was attributed to replating of dissolved gold from the working electrode on the counter electrode.

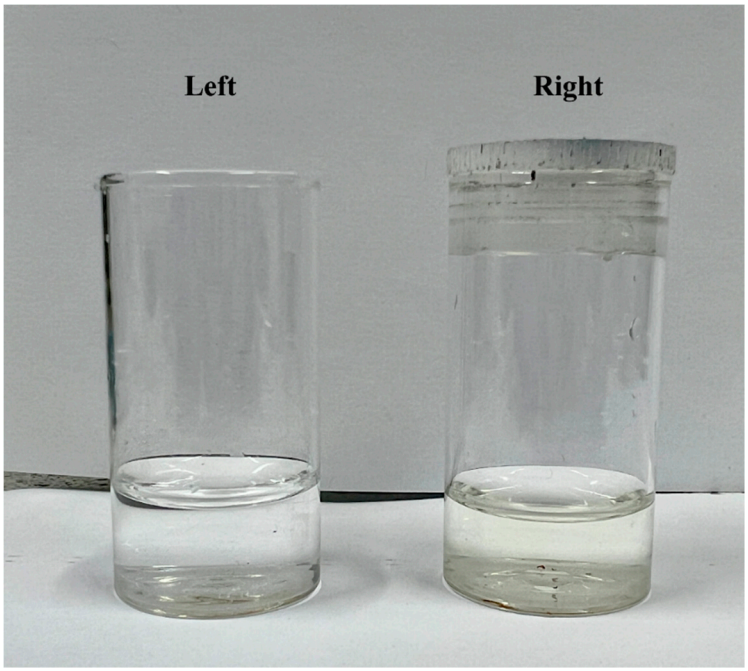

Figure S 2 A picture comparing ASW before and after multiple scan cyclic voltammetry being conducted. The start potential was −0.45 V vs MSE and swept towards 0.94 V before returning to −0.45 V. Left: original ASW; Right: ASW after 20 scans of CV.

Section 2: Calculation of Transfer Coefficients for the Chloride Oxidation from Tafel Analysis

This section reports the use of Tafel analysis for obtaining the transfer coefficient β for the chloride oxidation reaction at a Pt electrode and a GCE. Figure 2(a) illustrates cyclic voltammograms obtained using either a Pt electrode or a GCE in degassed ASW, with a scan rate of 100 mVs^{-1}. For a Pt electrode, the potential sweep started at −0.45 V vs MSE, and swept towards 1.2 V before returning to −0.45 V. For a GCE, the voltammogram started at the same potential of −0.45 V vs MSE, followed by an anodic sweep up to 2.0 V and then lower to −1.3 V before the sweep back to −0.45 V. These ranges were selected to ensure that both forward and reverse peaks of the redox reactions associated with the analytes, chloride and bromide, were clearly recorded. The dominant oxidation Peak 2 was observed at 0.94 V vs MSE using a Pt electrode and 1.66 V vs MSE using a GCE, with a related cathodic Peak 2'seen at 0.53 V vs MSE and −0.21 V vs MSE respectively. The insert shows a first oxidation peak (Peak 1) recorded at 0.59 V vs MSE using a Pt electrode and 0.86 V vs MSE using a GCE. According to the previous study [1], Peak 2 is attributed to the oxidation of chloride and Peak 1 is assigned to be the bromide oxidation with hypobromous acid ($HOBr/OBr^-$) being the possible product as reported by Yu *et al.* [2]. The Peak 2' corresponds to the reduction of the products from the chloride and bromide oxidation.

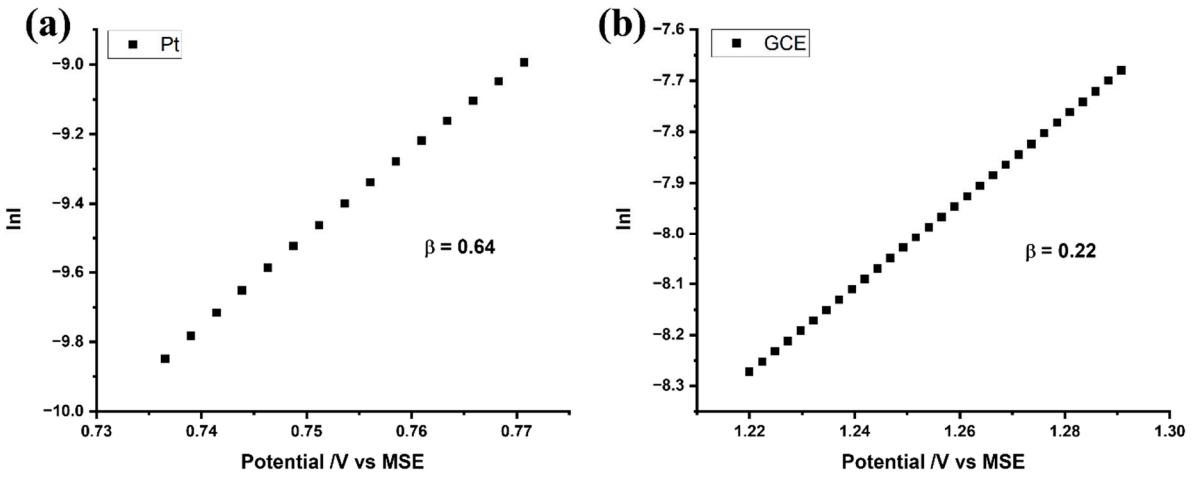

Figure S 3 The Tafel plots for the chloride oxidation in degassed ASW recorded at a scan rate of 100 mVs^{-1} (a) at a Pt electrode (b) at a GCE. 10% - 30% of the current range of the forward wave was used.

The Tafel analysis of Peak 2 was performed on the voltammograms starting from 10% to 30% of the peak height [3]. The transfer coefficient β was calculated from the following expression 1. [4-6]

$$\beta = \frac{RT}{F}\frac{\partial ln|I_{ox}|}{\partial E} \quad (1)$$

where I_{ox} is the oxidative current.

For the chloride oxidation in ASW recorded at a scan rate of 100 mVs^{-1} at a Pt electrode and a GCE, Tafel plots of $ln|I_{ox}|$ vs potential (V vs MSE) are shown as SI.3a and 3b respectively. The corresponding β value was calculated to be 0.64 ± 0.03 for a Pt electrode and 0.22 ± 0.03 for a GCE.

Section 3: Square Wave Voltammetry Applied to Bromide Oxidation

To obtain square wave voltammograms with the best resolution for potential analytical purposes, the optimisation of SWV parameters was conducted in a degassed ASW as shown in Figure S 4. Voltammograms were recorded starting at a potential of −0.45 V vs MSE and stopped at 1.3 V with a fixed step potential of 1 mV whilst varying the frequency and amplitude. Figure S 4 indicates that as the frequency increases, the signal at ca 0.8 V vs MSE becomes better defined with a higher peak current. A similar trend is observed by increasing the amplitude. Despite the minor improvement, the recorded signal overlaps the response from Peak 2 and also the solvent decomposition. Meanwhile, as with cyclic voltammetry, the presence of significant currents prior to the analytical signal indicates that a suitable baseline correction would be required for data analysis. Attention therefore returned to the cyclic voltametric data and standard additions made as described in the main text [7].

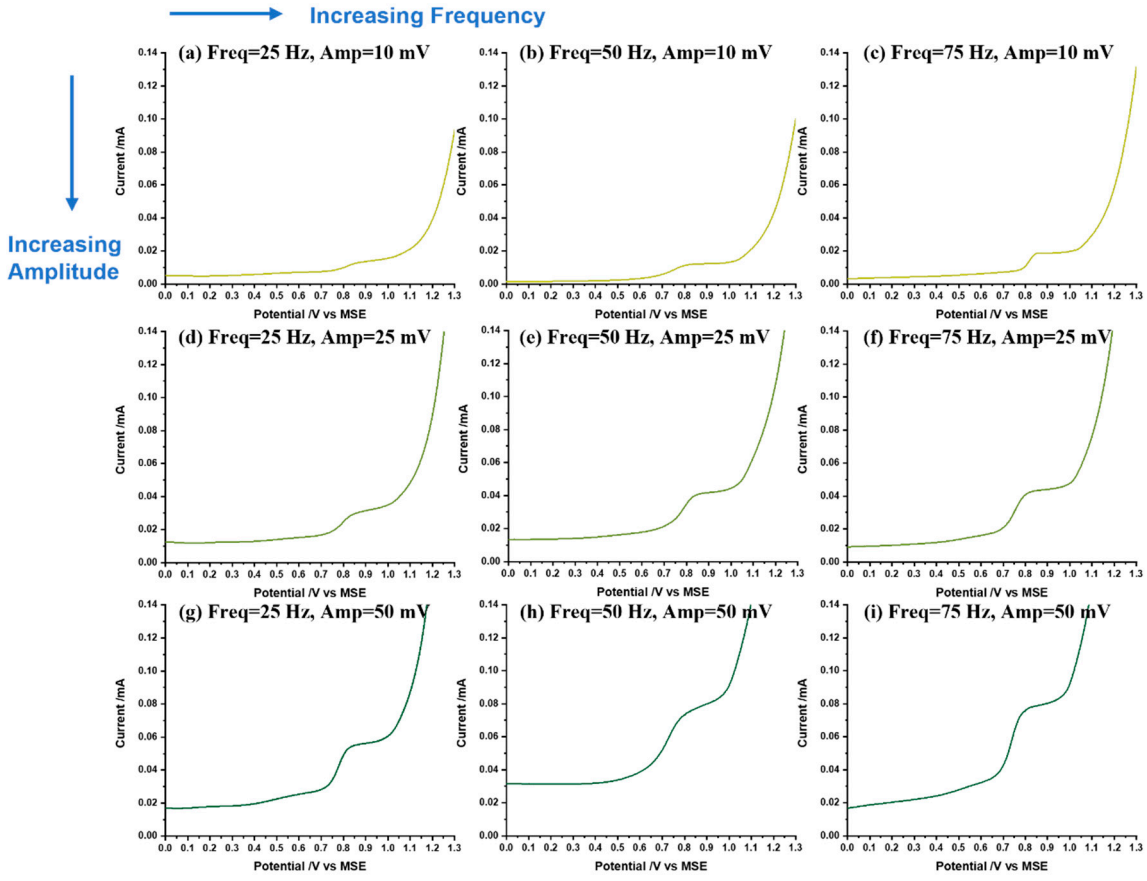

Figure S 4 Effect of increasing frequency (from left to right) and increasing amplitude (downward) on the SWV (focusing on bromide oxidation peak) with a step potential of 1 mV in a degassed ASW. (a) Freq = 25 mV, Amp = 10 mV, (b) Freq = 50 mV, Amp = 10 mV, (c) Freq = 75 mV, Amp = 10 mV, (d) Freq = 25 mV, Amp = 25 mV, (e) Freq = 50 mV, Amp = 25 mV, (f) Freq = 75 mV, Amp = 25 mV, (g) Freq = 25 mV, Amp = 50 mV, (h) Freq = 50 mV, Amp = 50 mV, (i) Freq = 75 mV, Amp = 50 mV.

Section 4: Method of Baseline Correction Applied to the Bromide Oxidation Voltammetry

To analyse the results of standard additions, voltammograms with the potential window focusing on Peak 1 were recorded as shown in Figure S 5 (black curves). Because of the pre-wave to Peak 1, a baseline correction was required for each measurement. This was made by extrapolating the pre-wave as shown by the red lines in Figure S 5 and subtracting the baseline from the experimental voltammogram to produce the corrected voltammograms shown in blue. The resultant voltammograms (blue curves) indicate a better-defined bromide oxidation signal and clear peak current of which was then used to plot Fig. 4b, showing the plot of peak current against the concentration of bromide added to the original ASW.

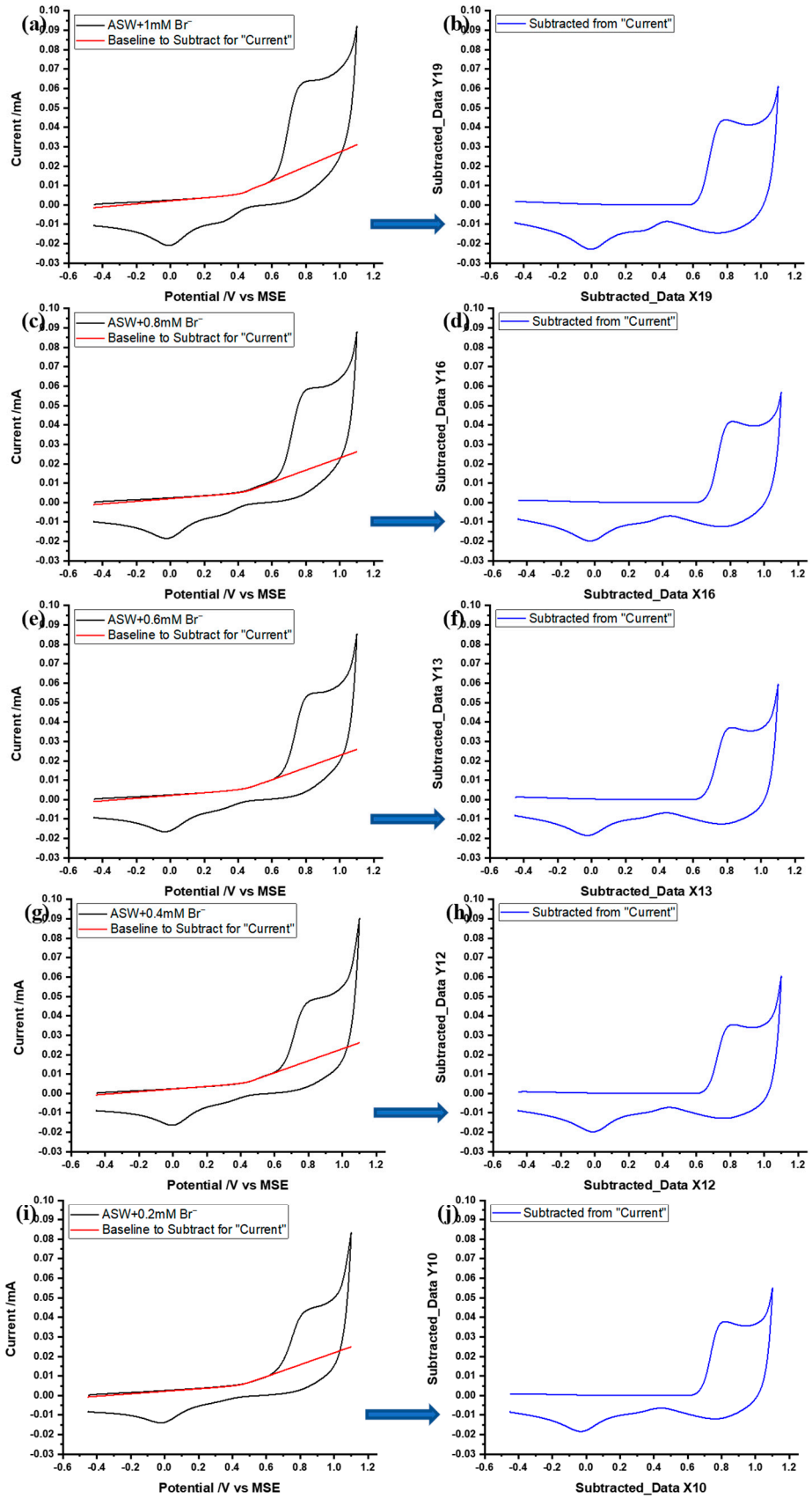

Figure S 5 The original voltammograms (black curve) and the modified voltammograms (blue curve) after a baseline correction (red line) obtained in degassed ASW with an addition of bromide concentration of (a-b) 0.2 mM, (c-d) 0.4 mM, (e-f) 0.6 mM, (g-h) 0.8 mM, (i-i) 1.0 mM. The baselines were selected as an extrapolation of the pre-wave.

Section 5: The Optimisation of SWV Parameters for Chloride Detection at a Pt Electrode

This section reports the optimisation of SWV parameters for chloride detection in degassed ASW as shown in Figure S 6. Voltammograms were recorded from a potential of −0.45 V vs MSE and stopped at 1.25 V with a fixed step potential of 1 mV whilst varying the frequency (5 – 25 Hz) and amplitude (10 – 50 mV). For comparison, the SWV with the same parameters was also conducted in 0.7 M $NaNO_3$ (dark lines) with the same ionic strength as seawater [8]. As the frequency increases, there is a higher chloride oxidation peak at ca 0.85 V vs MSE, but one can also notice that the effect of solvent breakdown gets more significant enhancing the current in the vicinity of the diffusion tail. Therefore, the frequency of 5 Hz was subsequently implemented in analytical measurements.

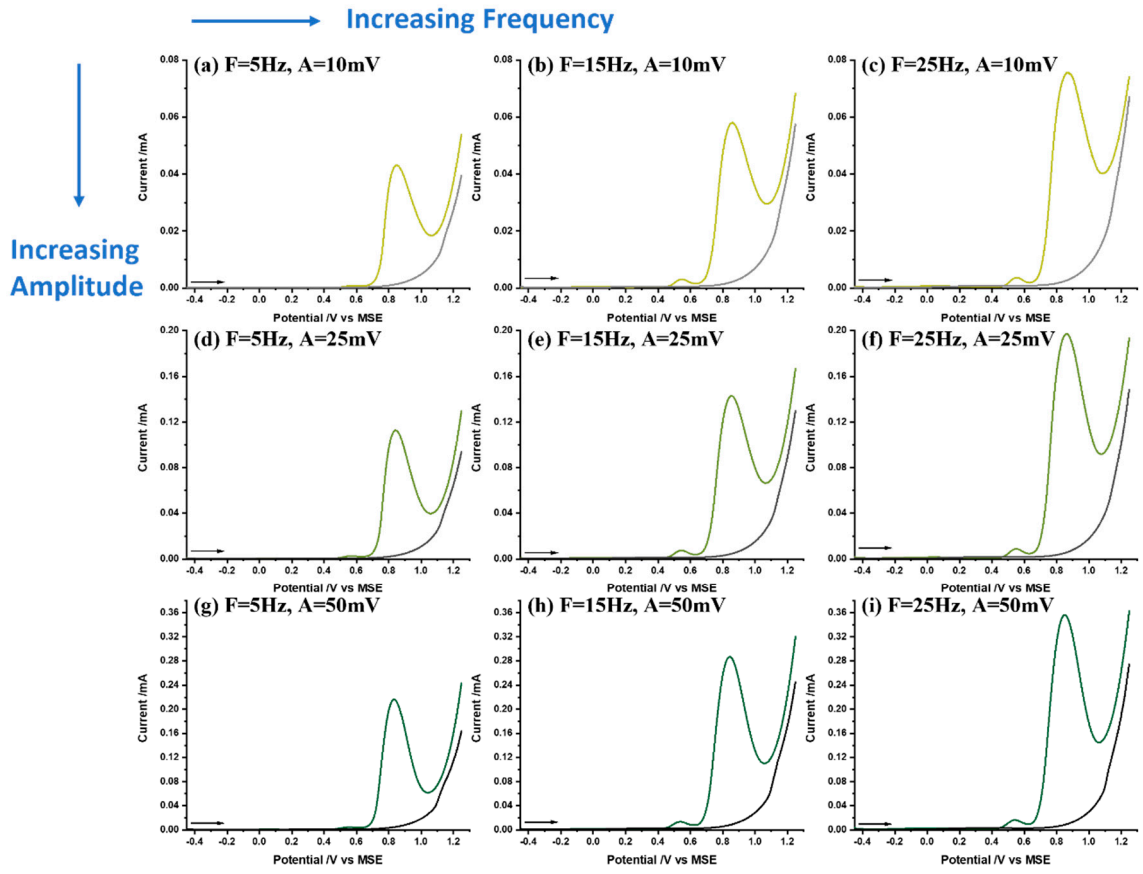

Figure S 6 Effect of increasing frequency (from left to right) and increasing amplitude (downward) on the SWV (focusing on chloride oxidation peak) with a step potential of 1 mV in degassed ASW. (a) Freq = 5 mV, Amp = 10 mV, (b) Freq = 10 mV, Amp = 10 mV, (c) Freq = 25 mV, Amp = 10 mV, (d) Freq = 5 mV, Amp = 25 mV, (e) Freq = 10 mV, Amp = 25 mV, (f) Freq = 25 mV, Amp = 25 mV, (g) Freq = 5 mV, Amp = 50 mV, (h) Freq = 15 mV, Amp = 50 mV, (i) Freq = 25 mV, Amp = 50 mV. All voltammograms are compared with data (dark lines) obtained in 0.7 M $NaNO_3$ with the same ionic strength as seawater [8].

In contrast to the frequency, there is no obvious difference in peak resolution by increasing the amplitude despite the higher peak current as shown in Figure S 6. To find the optimal amplitude

for chloride oxidation detection, the three amplitudes (10 mV, 25 mV and 50 mV) were assessed by further study in ASW containing various concentrations of chloride (0.484 M – 0.593 M) with the criteria being achieving the highest sensitivity and the best linearity. Figure S 7 (a-c) display the voltammograms obtained with the three different amplitudes respectively, from which it can be seen that the peak height of the chloride oxidation at 0.85 V vs MSE increases with the concentration of chloride. To analyse the data, the chloride oxidation peak currents were recorded. The plots of peak current against the chloride concentration in ASW samples are shown in Figure S 7d. We saw that an amplitude of 50 mV (blue dots) resulted in the highest sensitivity with the best linearity ($R^2 = 0.991$) compared to the other two. Therefore, the optimised SWV with a frequency of 5 Hz, an amplitude of 50 mV and a step potential of 1 mV was applied to record the electroanalytical responses of chloride ions in ASW and real sample analysis.

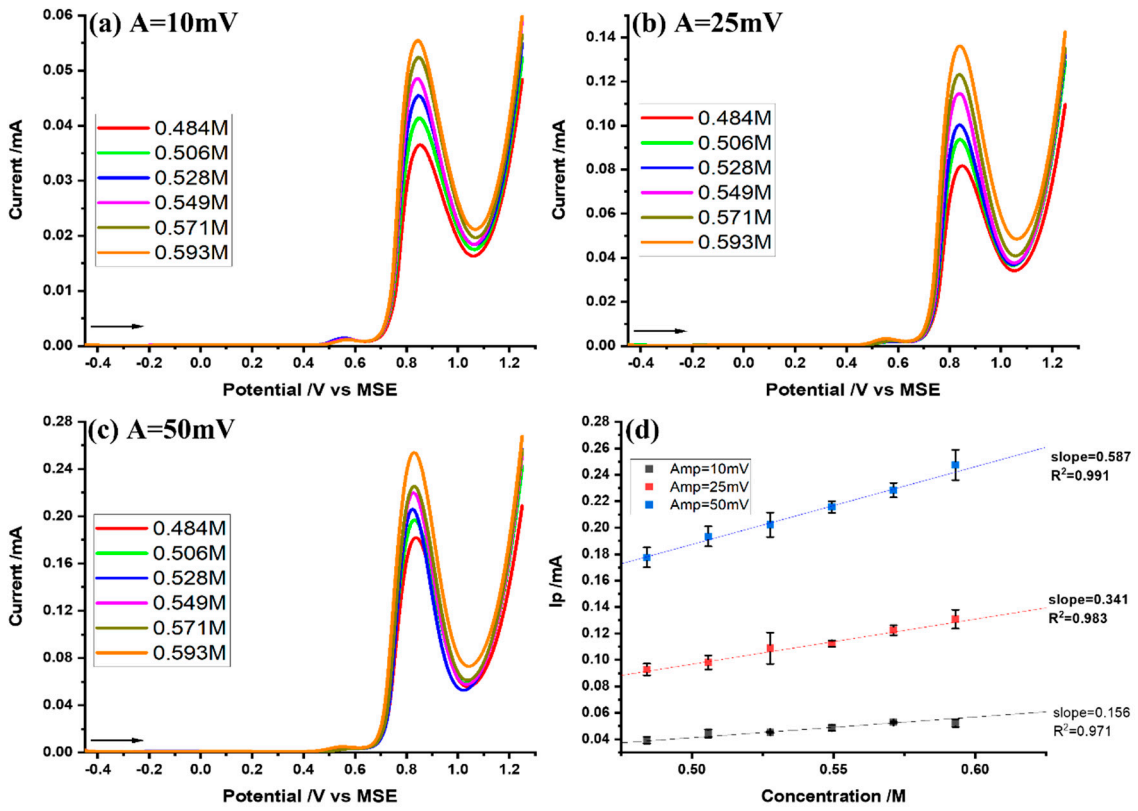

Figure S 7 Square wave voltammograms (step potential 1 mV, frequency 5 Hz) recorded at a Pt electrode in degassed ASW with various chloride concentrations of (0.484M-0.593M) with an amplitude of (a) 10 mV, (b) 25 mV and (c) 50 mV. See text for details of the scan range and the start potential. (d) The calibration curves of the resultant chloride oxidation peak heights against chloride concentrations. Amplitude = 10 mV (black dots); Amplitude = 25 mV (red dots); Amplitude = 50 mV (blue dots). Each data point consists of 3 repeats.

References:

1. Chen, Y.; Compton, R.G. A bespoke reagent-free amperometric bromide sensor for seawater. *Talanta* **2023**, *253*, 124019, doi:https://doi.org/10.1016/j.talanta.2022.124019.
2. Yu, J.; Yang, M.; Batchelor-McAuley, C.; Barton, S.; Rickaby, R.E.M.; Bouman, H.A.; Compton, R.G. Rapid Opto-electrochemical Differentiation of Marine Phytoplankton. *ACS Meas. Sci. Au* **2022**, *2*, 342-350, doi:https://doi.org/10.1021/acsmeasuresciau.2c00017.
3. Li, D.; Lin, C.; Batchelor-McAuley, C.; Chen, L.; Compton, R.G. Tafel analysis in practice. *Journal of Electroanalytical Chemistry* **2018**, *826*, 117-124, doi:https://doi.org/10.1016/j.jelechem.2018.08.018.
4. Compton, R.G.; Banks, C.E. *Understanding Voltammetry*; World Scientific, 3rd edition, 2018.
5. Guidelli, R.; Compton, R.G.; Feliu, J.M.; Gileadi, E.; Lipkowski, J.; Schmickler, W.; Trasatti, S. Defining the transfer coefficient in electrochemistry: An assessment (IUPAC Technical Report). *Pure Appl. Chem.* **2014**, *86*, 245-258, doi:https://doi.org/10.1515/pac-2014-5026.
6. Guidelli, R.; Compton, R.G.; Feliu, J.M.; Gileadi, E.; Lipkowski, J.; Schmickler, W.; Trasatti, S. Definition of the transfer coefficient in electrochemistry (IUPAC Recommendations 2014). *Pure Appl. Chem.* **2014**, *86*, 259-262, doi:https://doi.org/10.1515/pac-2014-5025.
7. Harris, D.C. *Quantitative chemical analysis*; Macmillan, 2010.
8. Millero, F.J. The Physical Chemistry of Seawater. *Annu. Rev. Earth Planet. Sci.* **1974**, *2*, 101-150, doi:https://doi.org/10.1146/annurev.ea.02.050174.000533.